Organic LETTERS

Letter

pubs.acs.org/OrgLett

Ullmann Reaction of Aryl Chlorides on Various Surfaces and the Application in Stepwise Growth of 2D Covalent Organic Frameworks

Ke Ji Shi,[†] Ding Wang Yuan,[‡] Cheng Xin Wang,[†] Chen Hui Shu,[†] Deng Yuan Li,[†] Zi Liang Shi,[§] Xin Yan Wu,[†] and Pei Nian Liu*[,†]

[†]Shanghai Key Laboratory of Functional Materials Chemistry, Key Lab for Advanced Materials and Institute of Fine Chemicals, East China University of Science and Technology, 130 Meilong Road, Shanghai 200237, China

[‡]School of Materials Science and Engineering, Hunan University, Changsha 410082, China

[§]Center for Soft Condensed Matter Physics & Interdisciplinary Research, Soochow University, No.1 Shizi Street, Suzhou, Jiangsu Province 215006, China

Supporting Information

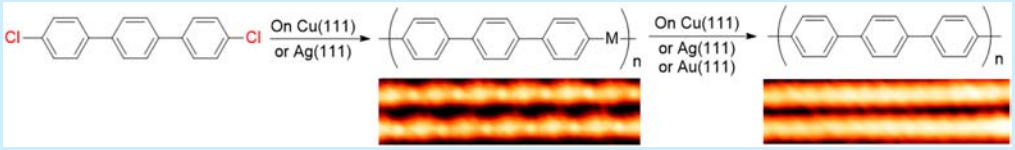

ABSTRACT: On-surface Ullmann coupling reaction of aryl chlorides has been achieved on Cu(111), Ag(111), and Au(111), and the mechanism has been investigated on the single molecule level using scanning tunneling microscopy and density functional theory. The different reactivity of the aryl halides was utilized to design a stepwise on-surface synthesis, which affords a zigzag template and then converts to 2D porous networks.

Two-dimensional covalent organic networks, known as covalent organic frameworks (COFs),[1] have attracted significant interest because of their numerous potential applications such as nanopatterning,[2] organic electronics,[3] nanoreactors,[4] and selective immobilization of functional molecules in specific pores.[5] Ever since the pioneering work of Grill et al. in 2007, on-surface synthesis of organic monomer-based COFs under ultrahigh vacuum (UHV) has emerged as a powerful bottom-up fabrication strategy, which has been the subject of intense atomic investigations using scanning tunneling microscopy (STM).[6] Of the various organic reactions achieved on surfaces under ultrahigh vacuum,[7] Ullmann reactions of aryl bromides and iodides have proven powerful for constructing diverse macromolecular systems, including polymeric chains,[8] hyperbranched oligomers,[9] graphene ribbons,[10] porous molecular networks,[11] super honeycomb frameworks,[12] and other stuctures.[13]

On-surface Ullmann reactions on metals involving aryl chlorides have not been reported, although the C−Au−C organometallic structure from aryl chlorides has been described.[14] Performing such coupling reactions would be a significant achievement because aryl chlorides are the most useful single class of halides in organic synthesis due to their wide diversity as commercially available compounds,[15] although they are much less reactive than other halide classes. Their low reactivity is often attributed to the strength of the C−Cl bond; for example, the bond dissociation energy of Ph−Cl (95 kcal/mol) is higher than that of Ph−Br (80 kcal/mol) and Ph−I (65 kcal/mol). The high strength of the C−Cl bond impedes oxidative addition to copper, which is a critical initial step in coupling reactions. After extensive efforts over decades, the activation of the strong C−Cl bond had been achieved to drive aryl chloride coupling in solution by the discovery of metal catalysts with bulky, electron-rich ligands such as P(Bu-t)$_3$ and PCy$_3$.[15,16]

Here we report the on-surface Ullmann reaction to form C−C covalent bonds on metals from aryl−Cl precursors (Scheme 1).[17]

Scheme 1. On-Surface Ullman Reactions of Aryl−Cl in This Work

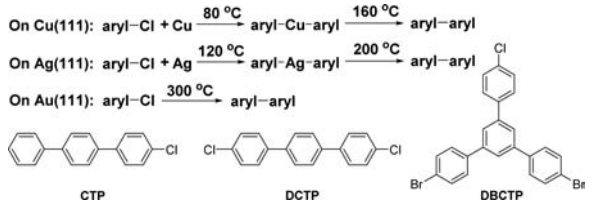

The compounds 4-chloro-1,1′:4′,1″-terphenyl (CTP) and 4,4″-dichloro-1,1′:4′,1″-terphenyl (DCTP) were used to form 0D or 1D chains. The ability and the mechanism of the single-crystal metallic surfaces Cu(111), Ag(111), and Au(111) to catalyze these Ullman reactions were studied at a single molecule level using STM and density functional theory (DFT) calculations. This protocol was used to achieve the stepwise reaction of 4,4″-dibromo-5′-(4-chlorophenyl)-1,1′:3′,1″-terphenyl (DBCTP) on

Received: January 21, 2016
Published: March 3, 2016

DOI: 10.1021/acs.orglett.6b00172
Org. Lett. 2016, 18, 1282−1285

Au(111), in which the different reactivities of aryl−Br and aryl−Cl were exploited.

In the first stage, CTP was deposited on Cu(111) at room temperature under ultrahigh vacuum, and the sample was annealed to 80 °C for 30 min. STM showed that CTP dimerized to form dumbbell-shaped structures comprising two large bright ovals and a smaller, less bright round dot in the middle (Figure 1a). The stick structure was 29.0 ± 0.5 Å long, consistent with the

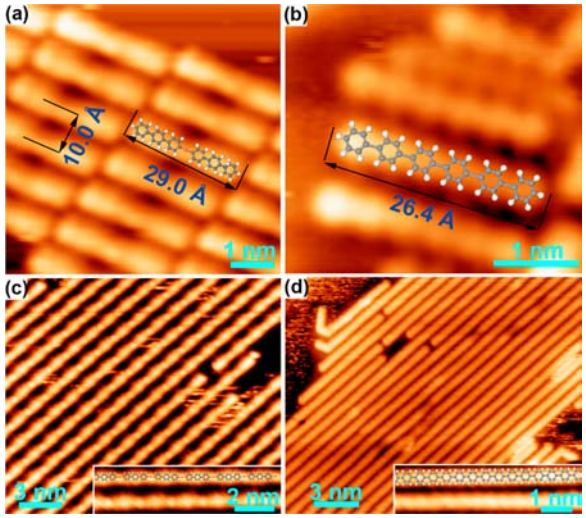

Figure 1. Molecules CTP and DCTP on a Cu(111) surface: (a) CTP after annealing at 80 °C (−1.6 V, −0.08 nA). (b) CTP after annealing at 160 °C (−1.5 V, −0.08 nA). (c) DCTP after annealing at 80 °C (−1.0 V, −0.07 nA). (d) DCTP after annealing at 160 °C (−1.0 V, −0.06 nA).

DFT-predicted length of 29.1 Å (Figure S9, SI). These results suggest that the stick structure is the oxidative addition intermediate $(Ph)_3$−Cu−$(Ph)_3$ occurring on the reaction pathway from $(Ph)_3$−Cl to the final product $(Ph)_6$.[18] These organometallic intermediates assembled side-by-side into an ordered, close-packed array with distance of 1.0 nm, mainly along the $[11\bar{2}]$ or equivalent directions on Cu(111).

The sample was annealed further to 160 °C for 30 min, and the high-resolution STM image revealed the formation of new dimers in which the discernible bright, round dot in the middle of $(Ph)_3$−Cu−$(Ph)_3$ intermediates disappeared and six uniform benzenes were resolved (Figure 1b). The dimers were 26.4 ± 0.5 Å long, which is shorter than the length of the $(Ph)_3$−Cu−$(Ph)_3$ intermediates and agrees with the DFT-predicted length of 26.6 Å for $(Ph)_6$ (Figure S10, SI). These results indicate that aryl chloride $(Ph)_3$−Cl underwent covalent coupling at 160 °C on Cu(111) to form $(Ph)_6$.

To identify the observed 1D chain structure, DCTP was deposited on Cu(111) held at room temperature, and the sample was annealed to 80 °C for 30 min. The high-resolution STM image showed that DCTP molecules were linked together into extended linear structures basically along the $[11\bar{2}]$ or equivalent directions of the substrate (Figure 1c). At a bias voltage of −1.0 V, the 1D chains exhibited a periodic structure, in which spindle-shaped features alternated with bright, round features. The distance between the two round dots was 15.8 ± 0.5 Å (Figure 1c, inset), in agreement with the DFT-predicted length of 15.4 Å (Figure S11, SI). The linear periodic structure appears to correspond to the organometallic intermediate in which $(Ph)_3$ units alternate with Cu atoms. This is similar to the reaction of Br−$(Ph)_3$−Br on Cu(111),[18] indicating that the same organometallic intermediates are produced from Cl−$(Ph)_3$−Cl and Br−$(Ph)_3$−Br.

Further annealing of the sample to 160 °C for 30 min led to the disappearance of bright round dots in organometallic intermediates and to the formation of homogeneous chainlike oligomers with occasional branched structures (Figure 1d). Individually linked benzenes were resolved by STM (Figure 1d, inset), with two adjacent benzenes lying 4.2 Å apart (line profile, see Figure S8, SI). Topographic features of the oligomers suggest that covalent coupling of Cl−$(Ph)_3$−Cl occurred at 160 °C on Cu(111) to form poly(*p*-phenylene) in linear chains that were sometimes longer than 50 nm. These chains grew basically along the $[11\bar{2}]$ or equivalent directions of the substrate with chain distance of 0.9 nm.

After conducting these experiments on Cu(111), we examined the ability of Ag(111) to catalyze similar Ullmann reactions. DCTP was deposited on Ag(111) held at 25 °C and annealed at various temperatures. Linear chains formed at annealing temperatures up to 120 °C. These results suggest that Ag(111) activates aryl chloride less strongly than Cu(111) to form organometallic intermediates. On the Ag(111) surface, DCTP molecules were linked together periodically as linear structures in which dim, spindle-shaped $(Ph)_3$ groups alternated with brighter, round Ag atoms (Figure 2a). We assigned the linear periodic

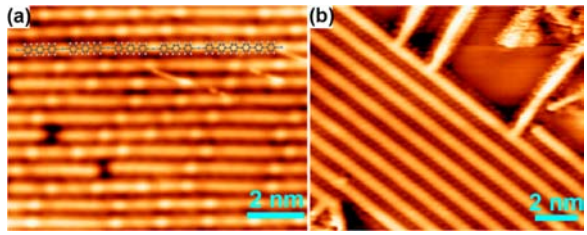

Figure 2. DCTP on a Ag(111) surface: (a) DCTP after annealing at 120 °C (−2.5 V, −0.12 nA); (b) DCTP after annealing at 200 °C (2.5 V, 0.04 nA).

structure as the silver organometallic intermediate, in which most $(Ph)_3$ fragments were linked to an adjacent Ag atom. This is similar to the organometallic intermediate that forms from Br−$(Ph)_3$−Br on Ag(111).[20] In addition to periodic single-$(Ph)_3$ fragments, fragments containing two to three $(Ph)_3$ fragments were observed in the linear structures. These longer fragments are likely early stages of the final product, poly(*p*-phenylene) oligomers. The structural features of these various species were even clearer at a bias voltage of 2.5 V: poly(*p*-phenylene) oligomers appeared as bright sticks or ovals and Ag atoms as smaller, less bright dots (Figure S6).

Annealing the sample further to 200 °C for 30 min caused the linear periodic structures to disappear and the $(Ph)_3$ units to connect to each other via C−C bonds, generating aligned linear chains with occasional branches (Figure 2b). Some covalent chains were more than 50 nm long. The distance between adjacent chains was 1.0 nm, and the round dots appeared in orderly lines; we assigned the dots to be Cl atoms dissociated from DCTP.

A previous report of Br−$(Ph)_3$−Br homocoupling on Au(111) suggested that the C−Au−C intermediate was unstable;[21] therefore, we deposited DCTP molecules onto Au(111) at 25 °C and then annealed the sample to 200 °C for 30 min. Only short chains of poly(*p*-phenylene) were generated, with most oligomers containing two to three $(Ph)_3$ fragments (Figure 3a).

DOI: 10.1021/acs.orglett.6b00172
Org. Lett. 2016, 18, 1282−1285

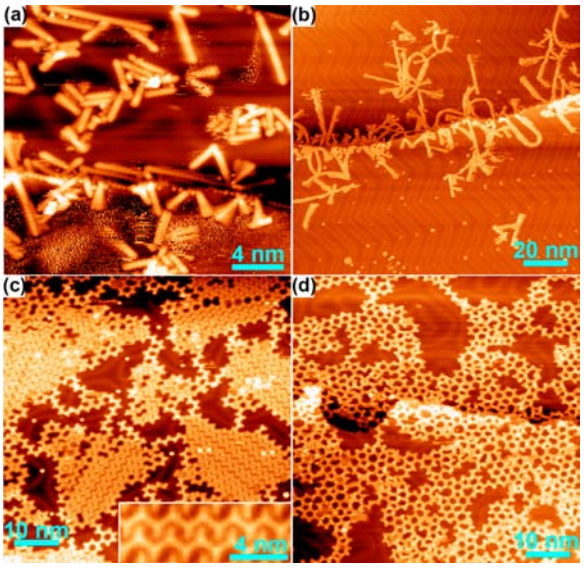

Figure 3. DCTP and BCB on an Au(111) surface: (a) DCTP after annealing at 200 °C (−1.0 V, −0.09 nA); (b) DCTP after annealing at 300 °C (−2.5 V, −0.08 nA); (c) BCB after being deposited on Au(111) held at 200 °C (−1.5 V, −0.07 nA); (d) BCB after annealing at 300 °C (−2.0 V, −0.08 nA).

Some oligomers contained six to eight $(Ph)_3$ fragments, and these usually lay along the step edge, where the surface shows greater ability to activate the reaction. Some chains exhibited multiple features that appeared to arise from the shifting of chain ends during STM imaging. These multiple features were not observed on Cu(111) or Ag(111), perhaps reflecting weaker adsorption energy of Au(111). Further annealing the sample to 300 °C for 30 min led to much longer oligomeric chains, with some chains containing more than 20 $(Ph)_3$ units (Figure 3b). Interestingly, most chains grew with one end attached to the step edges of the substrate and did not strictly follow any crystalline orientations of the Au(111) substrate. Many chains were curved, implying that the poly(*p*-phenylene) oligomers are highly flexible. By contrast, the coupling of aryl chloride on an insulating calcite surface can be achieved at 337 °C.[17]

In on-surface syntheses, the nonreversibility of covalent bond formation causes kinetic trapping during polymerization. As the result, macromolecular systems formed in on-surface syntheses usually lack long-range order, contain structural defects or exhibit a broad size distribution. Various strategies have been proposed to overcome this obstacle,[7e,g,17,22] including the hierarchical polymerization.[23] We addressed this problem by taking advantage of the substantial difference in reactivity between aryl chlorides and aryl bromides. We designed a DBCTP molecule containing one chloride end and two bromide ends, which we could use in stepwise on-surface synthesis to generate a template and subsequently form 2D porous networks.

DBCTP molecules were deposited on Au(111) held at 200 °C, and zigzag chains formed preferentially along $[11\bar{2}]$ or equivalent orientations of the substrate, further aggregating into well-ordered 2D islands. The bend-to-bend distance in the *m*-terphenylene units was 21.3 ± 0.2 Å (Figure 3c), indicating that the two phenyl bromide ends of BCB had formed C−C bonds,[19] while the phenyl chloride end remained intact. This result illustrates that the stronger interaction of the zigzag chain with the surface causes lower mobility and thus remarkably prohibits the reaction of the phenyl chloride end, in comparison with the reaction of free-moving DCTP on Au(111). Adjacent zigzag chains were 1.56 nm apart (Figure 3c), suggesting weak van der Waals interactions between chains. In contrast, depositing DBCTP molecules onto Au(111) held at room temperature followed by annealing to 200 °C afforded only triangular islands (10 nm) comprising tangled chains.

When DBCTP molecules deposited on Au(111) at 200 °C were further heated to 300 °C, the phenyl chloride ends in the zigzag template underwent coupling to afford a porous network comprising mainly hexagon structures together with some pentagon and heptagon structures (Figure 3d). In this way, our approach allowed sequential activation of phenyl bromide and phenyl chloride sites in DBCTP to form C−C bonds in a stepwise manner. The resulting polymer network was much more uniform than the networks produced on Au(111) using 1,3,5-tris(4-bromophenyl)benzene[24] or 1,3,5-tris(4-chlorophenyl)benzene (Figure S7).

Considering the second step of the coupling reaction of aryl chlorides is same with those of aryl bromides and aryl iodines,[25a] we compared the abilities of the three metal surfaces to catalyze the first dechlorination step of aryl chlorides in Ullman coupling. We analyzed dechlorination reactions using the climbing image nudged elastic band (CI-NEB) technique combined with the dimer method implemented in the plane-wave based Vienna ab initio simulation package (VASP).[25] As shown in Figure 4,

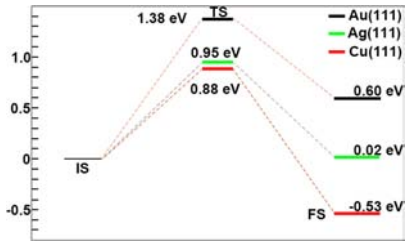

Figure 4. Calculated energy diagrams of dechlorination of phenyl chloride on Cu(111), Ag(111), and Au(111). $E_{barrier}$ and E_{react} were defined as, respectively, $(E_{TS} - E_{IS})$ and $(E_{FS} - E_{IS})$.

calculated reaction barrier ($E_{barrier}$) and reaction energy (E_{react}) values (eV) for phenyl chloride dissociation were 0.88 and −0.53 on Cu(111), 0.95 and 0.02 on Ag(111), and 1.38 and 0.60 on Au(111). Higher calculated $E_{barrier}$ value on Au(111) than on Ag(111) and Cu(111) is consistent with the observed reaction temperature tendency of aryl chloride in our experiments. These energy barriers to dechlorination on metal surfaces are much lower than in the gas phase (4.51 eV), indicating that the metals strongly activate aryl chlorides. Moreover, the calculated E_{react} values reveal that the reaction on Cu(111) is highly exothermic, and the reaction on Au(111) is highly endothermic. The different reaction enthalpies affect the reversibility of the first step of coupling to generate the organometallic intermediates and are consistent with the stability of copper organometallic intermediate and the instability of gold organometallic intermediate. In addition, the calculated $E_{barrier}$ and E_{react} values (eV) for phenyl bromide dissociation were 0.64 and −0.66 on Cu(111) (Figure S15, SI), which are consistent with the less active property of aryl chloride in comparison with aryl bromide.[25b]

In summary, we report here the on-surface Ullmann coupling reaction of aryl chlorides, which we analyzed in single molecule level using STM measurements and DFT calculations. On Cu(111) and Ag(111), aryl chlorides undergo coupling at much higher temperatures than aryl bromides to generate organo-

DOI: 10.1021/acs.orglett.6b00172
Org. Lett. 2016, 18, 1282−1285

metallic intermediates, which then convert to C−C linked products at elevated temperature. On Au(111), the aryl chlorides directly convert to the final C−C-linked products under much higher temperature than for aryl bromides. Taking advantage of the substantial difference in reactivity between aryl chlorides and bromides, we achieved a stepwise on-surface synthesis[23a] in which aryl bromides first coupled to form the C−C linked template and then aryl chlorides coupled to form 2D porous networks. This protocol for on-surface synthesis may allow bottom-up, hierarchical fabrication of conjugated nanostructures based on selective, sequential activation of aryl iodides, bromides, and chlorides.

■ ASSOCIATED CONTENT

Supporting Information

The Supporting Information is available free of charge on the ACS Publications website at DOI: 10.1021/acs.orglett.6b00172.

Synthesis and NMR spectra of the molecules, experimental and calculation procedures, and results (PDF)

■ AUTHOR INFORMATION

Corresponding Author

*E-mail: liupn@ecust.edu.cn.

Notes

The authors declare no competing financial interest.

■ ACKNOWLEDGMENTS

We thank Prof. Nian Lin in the Hong Kong University of Science & Technology and Prof. Wilson Ho in the University of California, Irvine for help with this work. This research was supported by the NSFC/China (Project Nos. 21421004, 21190033, 21561162003 and 21372072), the Eastern Scholar Distinguished Professor Program, the Programme of Introducing Talents of Discipline to Universities (B16017), the NCET (NCET-13-0798), the Basic Research Program of the Shanghai Committee of Science and Technology (Project No. 13M1400802), and the Fundamental Research Funds for the Central Universities.

■ REFERENCES

(1) Perepichka, D. F.; Rosei, F. *Science* **2009**, *323*, 216.

(2) Joo, S. H.; Choi, S. J.; Oh, I.; Kwak, J.; Liu, Z.; Terasaki, O.; Ryoo, R. *Nature* **2001**, *412*, 169.

(3) (a) Spitler, E. L.; Dichtel, W. R. *Nat. Chem.* **2010**, *2*, 672. (b) Wan, S.; Guo, J.; Kim, J.; Ihee, H.; Jiang, D. *Angew. Chem., Int. Ed.* **2008**, *47*, 8826.

(4) Lei, S.; Tahara, K.; Adisoejoso, J.; Balandina, T.; Tobe, Y.; De Feyter, S. *CrystEngComm* **2010**, *12*, 3369.

(5) Griessl, S. J. H.; Lackinger, M.; Jamitzky, F.; Markert, T.; Hietschold, M.; Heckl, W. M. *Langmuir* **2004**, *20*, 9403.

(6) Grill, L.; Dyer, M.; Lafferentz, L.; Persson, M.; Peters, M. V.; Hecht, S. *Nat. Nanotechnol.* **2007**, *2*, 687.

(7) (a) Sun, Q.; Zhang, C.; Li, Z.; Kong, H.; Tan, Q.; Hu, A.; Xu, W. *J. Am. Chem. Soc.* **2013**, *135*, 8448. (b) Gao, H.-Y.; Wagner, H.; Zhong, D.; Franke, J.-H.; Studer, A.; Fuchs, H. *Angew. Chem., Int. Ed.* **2013**, *52*, 4024. (c) Zhang, Y.-Q.; Kepčija, N.; Kleinschrodt, M.; Diller, K.; Fischer, S.; Papageorgiou, A. C.; Allegretti, F.; Björk, J.; Klyatskaya, S.; Klappenberger, F.; Ruben, M.; Barth, J. V. *Nat. Commun.* **2012**, *3*, 1286. (d) Zhou, H.; Liu, J.; Du, S.; Zhang, L.; Li, G.; Zhang, Y.; Tang, B. Z.; Gao, H.-J. *J. Am. Chem. Soc.* **2014**, *136*, 5567. (e) Zhong, D.; Franke, J.-H.; Podiyanachari, S. K.; Blömker, T.; Zhang, H.; Kehr, G.; Erker, G.; Fuchs, H.; Chi, L. *Science* **2011**, *334*, 213. (f) Zwaneveld, N. A. A.; Pawlak, R.; Abel, M.; Catalin, D.; Gigmes, D.; Bertin, D.; Porte, L. *J. Am. Chem. Soc.* **2008**, *130*, 6678. (g) Dienstmaier, J. F.; Medina, D. D.; Dogru, M.; Knochel, P.; Bein, T.; Heckl, W. M.; Lackinger, M. *ACS Nano* **2012**, *6*, 7234. (h) Gao, H.-Y.; Held, P. A.; Knor, M.; Mück-Lichtenfeld, C.; Neugebauer, J.; Studer, A.; Fuchs, H. *J. Am. Chem. Soc.* **2014**, *136*, 9658. (i) Weigelt, S.; Busse, C.; Bombis, C.; Knudsen, M. M.; Gothelf, K. V.; Strunskus, T.; Wöll, C.; Dahlbom, M.; Hammer, B.; Lægsgaard, E.; Besenbacher, F.; Linderoth, T. R. *Angew. Chem., Int. Ed.* **2007**, *46*, 9227. (j) Weigelt, S.; Busse, C.; Bombis, C.; Knudsen, M. M.; Gothelf, K. V.; Lægsgaard, E.; Besenbacher, F.; Linderoth, T. R. *Angew. Chem., Int. Ed.* **2008**, *47*, 4406.

(8) (a) Lipton-Duffin, J. A.; Ivasenko, O.; Perepichka, D. F.; Rosei, F. *Small* **2009**, *5*, 592. (b) Lipton-Duffin, J. A.; Miwa, J. A.; Kondratenko, M.; Cicoira, F.; Sumpter, B. G.; Meunier, V.; Perepichka, D. F.; Rosei, F. *Proc. Natl. Acad. Sci. U. S. A.* **2010**, *107*, 11200. (c) Lin, T.; Shang, X.; Adisoejoso, J.; Liu, P.; Lin, N. *J. Am. Chem. Soc.* **2013**, *135*, 3576.

(9) Wang, S.; Wang, W.; Lin, N. *Phys. Rev. B: Condens. Matter Mater. Phys.* **2012**, *86*, 045428.

(10) Cai, J.; Ruffieux, P.; Jaafar, R.; Bieri, M.; Braun, T.; Blankenburg, S.; Muoth, M.; Seitsonen, A. P.; Saleh, M.; Feng, X.; Müllen, K.; Fasel, R. *Nature* **2010**, *466*, 470.

(11) (a) Gutzler, R.; Walch, H.; Eder, G.; Kloft, S.; Heckl, W. M.; Lackinger, M. *Chem. Commun.* **2009**, *45*, 4456. (b) Schlogl, S.; Sirtl, T.; Eichhorn, J.; Heckl, W. M.; Lackinger, M. *Chem. Commun.* **2011**, *47*, 12355. (c) Faury, T.; Clair, S.; Abel, M.; Dumur, F.; Gigmes, D.; Porte, L. *J. Phys. Chem. C* **2012**, *116*, 4819.

(12) Bieri, M.; Treier, M.; Cai, J.; Ait-Mansour, K.; Ruffieux, P.; Groning, O.; Groning, P.; Kastler, M.; Rieger, R.; Feng, X.; Mullen, K.; Fasel, R. *Chem. Commun.* **2009**, *45*, 6919.

(13) (a) Mendez, J.; Lopez, M. F.; Martin-Gago, J. A. *Chem. Soc. Rev.* **2011**, *40*, 4578. (b) Lackinger, M.; Heckl, W. M. *J. Phys. D: Appl. Phys.* **2011**, *44*, 464011.

(14) Zhang, H.; Franke, J.-H.; Zhong, D.; Li, Y.; Timmer, A.; Arado, O. D.; Mönig, H.; Wang, H.; Chi, L.; Wang, Z.; Müllen, K.; Fuchs, H. *Small* **2014**, *10*, 1361.

(15) Littke, A. F.; Fu, G. C. *Angew. Chem., Int. Ed.* **2002**, *41*, 4176.

(16) Fu, G. C. *Acc. Chem. Res.* **2008**, *41*, 1555.

(17) Kittelmann, M.; Nimmrich, M.; Lindner, R.; Gourdon, A.; Kühnle, A. *ACS Nano* **2013**, *7*, 5614.

(18) (a) Wang, W.; Shi, X.; Wang, S.; Van Hove, M. A.; Lin, N. *J. Am. Chem. Soc.* **2011**, *133*, 13264. (b) Di Giovannantonio, M.; El Garah, M.; Lipton-Duffin, J.; Meunier, V.; Cardenas, L.; Fagot Revurat, Y.; Cossaro, A.; Verdini, A.; Perepichka, D. F.; Rosei, F.; Contini, G. *ACS Nano* **2013**, *7*, 8190.

(19) Fan, Q.; Wang, C.; Han, Y.; Zhu, J.; Hieringer, W.; Kuttner, J.; Hilt, G.; Gottfried, J. M. *Angew. Chem., Int. Ed.* **2013**, *52*, 4668.

(20) Chung, K.-H.; Koo, B.-G.; Kim, H.; Yoon, J. K.; Kim, J.-H.; Kwon, Y.-K.; Kahng, S.-J. *Phys. Chem. Chem. Phys.* **2012**, *14*, 7304.

(21) Basagni, A.; Sedona, F.; Pignedoli, C. A.; Cattelan, M.; Nicolas, L.; Casarin, M.; Sambi, M. *J. Am. Chem. Soc.* **2015**, *137*, 1802.

(22) (a) Dienstmaier, J. F.; Gigler, A. M.; Goetz, A. J.; Knochel, P.; Bein, T.; Lyapin, A.; Reichlmaier, S.; Heckl, W. M.; Lackinger, M. *ACS Nano* **2011**, *5*, 9737. (b) Guan, C.-Z.; Wang, D.; Wan, L.-J. *Chem. Commun.* **2012**, *48*, 2943. (c) Weigelt, S.; Bombis, C.; Busse, C.; Knudsen, M. M.; Gothelf, K. V.; Lægsgaard, E.; Besenbacher, F.; Linderoth, T. R. *ACS Nano* **2008**, *2*, 651.

(23) (a) Lafferentz, L.; Eberhardt, V.; Dri, C.; Africh, C.; Comelli, G.; Esch, F.; Hecht, S.; Grill, L. *Nat. Chem.* **2012**, *4*, 215. (b) Eichhorn, J.; Strunskus, T.; Rastgoo-Lahrood, A.; Samanta, D.; Schmittel, M.; Lackinger, M. *Chem. Commun.* **2014**, *50*, 7680. (c) Eichhorn, J.; Nieckarz, D.; Ochs, O.; Samanta, D.; Schmittel, M.; Szabelski, P. J.; Lackinger, M. *ACS Nano* **2014**, *8*, 7880.

(24) Blunt, M. O.; Russell, J. C.; Champness, N. R.; Beton, P. H. *Chem. Commun.* **2010**, *46*, 7157.

(25) (a) Nguyen, M.-T.; Pignedoli, C. A.; Passerone, D. *Phys. Chem. Chem. Phys.* **2011**, *13*, 154. (b) Björk, J.; Hanke, F.; Stafström, S. *J. Am. Chem. Soc.* **2013**, *135*, 5768.

DOI: 10.1021/acs.orglett.6b00172
Org. Lett. 2016, 18, 1282−1285